

## Synthesis of Disodium Silicon Triscatecholate from Silica

Kanda Wongwailikhit<sup>1\*</sup>, Praifon Puangsing<sup>1</sup> and Yochio Kabe<sup>2</sup>

<sup>1</sup>Department of Chemistry, Faculty of Science, Rangsit University, Pathumthani, Thailand

<sup>2</sup>Department of Chemistry, Faculty of Science, Kanagawa University, Tsuchiya, Hiratsuka-shi, Kanagawa, Japan

\*Correspondence author (email: kanda.w@rsu.ac.th)

Triscatecholate is one of the anchor molecules imitating tripodal catecholate assemblies in mussel adhesion proteins and siderophores. These assemblies are biomimetic approaches inspired by natural multivalent metal binders. In this work, disodium silicon triscatecholate,  $\text{Na}_2[\text{Si}(\text{catecholate})_3]$ , was synthesized from the reaction between pyrocatechol (limiting agent) and sodium metasilicate nonahydrate at the mole ratio of 3:1. Two different reaction temperatures, 110°C and room temperature, were tested on two different concentrations of pyrocatechol (0.7247 and 2.7338 mole/L) at the same ratio as that of sodium metasilicate. It was proved by the <sup>1</sup>H-NMR spectrum that disodium silicon triscatecholate could be formed at room temperature. However, the product under a high temperature of 110°C provided a high purity product with fewer impurities compared with that under room temperature. At 110°C, the reaction at the lower concentration reduced the possible side reactions compared with the high concentration condition as water would take an important role in the reaction pathway.

**Key words:** Triscatecholate; disodium silicon triscatecholate; pyrocatechol; silicon siderophores

*Received: March 2022; Accepted: April 2022*

Recently, catecholates, one of the suitable anchor molecules, have been of interest for biomedically relevant metal surfaces and nanoparticles [1,2]. Catechol-type ligands are bifunctional organic molecules that very strongly bind onto metal oxides by forming complexes through adjacent phenolic —OH groups [3]. Many biological materials such as mussel byssus cuticle and mutilid threads are composed of those hierarchical metal complexes supporting the important behaviors like adhesive, frictional properties benefit, and many more. The complexes of catecholate can be applied as the continuous grafted material that can be tunably immobilized with other materials in the vicinity of a neutral or slightly acidic medium. Due to the electron deficiency of centered multivalent metal atoms, catecholate complexes are capable of acting as binding materials. It can also be used for immobilizing the binders as it delivers attractive anchors for durable immobilizations on metal surfaces. Franzmann et al (2011) reported the potential of the binded catecholates with non-peptidic trimeric that can form the stable molecular monolayers at the surface of Titanium dioxide and stainless steel [4].

The centered metal atom of catecholate is often composed of silica [5], zinc [6], alumina, zirconia, iron [7], and titania [8] that can enhance the enzyme catalytic properties [9,10]. For instance, it was reported that the complex of Fe-catecholate (1,2-dihydroxybenzene) takes part in the mussel byssus

cuticles and provides flexible lasting properties [11]. Among those metals, silica complexes of catecholates were reported to be one of the alternative candidates as enzyme supports for bacterial siderophores that can be used in antibacterial applications due to their appropriate properties [2,9,12,13]. Firstly, the high acidic property of silica catecholates has the capability to support the catalytic activity in the organic synthesis reactions such as the hydrosilylation of aldehyde due to the strongly electron-withdrawing properties. Secondly, the decent thermal stability of the silica complex also provides high mechanical properties for enzyme support. Moreover, the visible light absorption property can enhance the photo-excitation in metal oxide, which can be further used as an alternative semiconductor.

One of the interesting applications of silicon catecholate is the bone-tissue engineering application that used the combination of silicon catecholate and collagen [14]. Sarker et al. studied the synthesis of silica/collagen composite from inorganic bioactive material and collagen [15] and reported that the greater the ratio of silica to collagen, the higher the compressive modulus for the scaffolds but lesser biocompatibility. They also suggested that the combination between Silica and collagen yielded high impacts in many applications not only biological applications but also the usage for environmental issues, delivery matters, and sensing [14]. Therefore, many attempts have fabricated the hypervalent silica-

based biopolymer using Silicon catecholate as the primary precursor such as the organosilanes [14], thiocyanates [16], and others [6,7].

Many successful syntheses of hypervalent tris(catecholato)silicate ion,  $[(C_6H_4O_2)_3Si]^{2-}$  with different counter cations have been recently reported. The counter ions include diethylammonium(I), triethylammonium(II), diisopropylammonium(III), morpholinium(IV), piperazinium(V), N-methylpiperazinium(VI), isopropylammonium, n-butylammonium, cyclohexylammonium, benzylammonium, and diisobutylammonium. Even though high percentages of yield were achieved by many researchers, most of them used expensive reactants like tetraethyl orthosilicate (TEOS) in their work [17].

Therefore, in this work, the authors aim to develop silicon catecholate using low-cost silica. The effector-conjugates of tripodal catecholates disodium triscatecholate were synthesized from pyrocatechol and sodium silicate. This low cost of disodium silicon triscatecholate is expected to be an alternative to produce the tripodal motif binder such as mussel adhesion proteins and siderophores.

## MATERIALS AND METHODS

### 1. Materials

Sodium metasilicate nonahydrate ( $Na_2SiO_3 \cdot 9H_2O$ ) (FUJIFILM, AR grade); pyrocatechol ( $C_6H_4(OH)_2$ ) (Wako, analytical grade); Dioxane (FUJIFILM, analytical grade); Ethyl acetate (EtOAc) (Wako, analytical grade); methanol (MeOH) (FUJIFILM, analytical grade); Diethyl ether ( $Et_2O$ ) (Wako, analytical grade); acetone (Wako, Analytical grade); sodium sulfate ( $Na_2SO_4$ ) (FUJIFILM, analytical grade); hexane (Wako, Analytical grade); Tetrahydrofuran (THF) (FUJIFILM, Analytical grade); were used as chemicals and solvents in this work. Methanol- $d_4$ , MagniSolv™, NMR grade, was for the  $^1H$ -NMR analysis. The reactions were conducted under an argon environment. Thin-layer chromatography was used as a simple technique for testing the formation of the

products at different times.  $^1H$ -NMR spectra were recorded on a JEOL JNM-ECS 400 instrument (400 MHz) in Deuterated methanol ( $CD_3OD$ ).

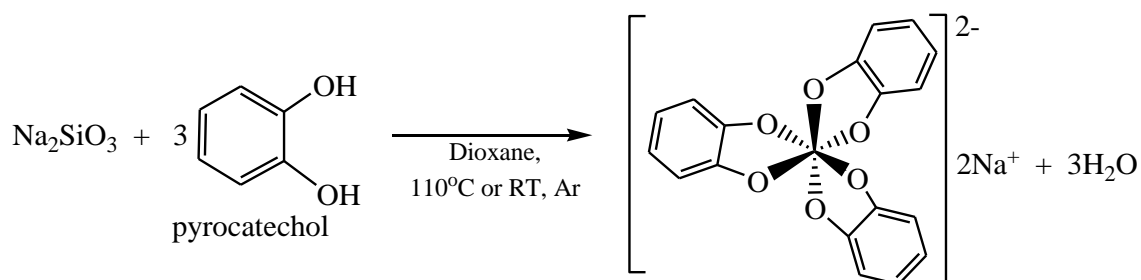
### 2. Methods

A solution of 0.7247 mole/L pyrocatechol in dioxane was dropwise into the solution of 0.2800 mole/L of  $Na_2SiO_3$  in distilled water. The mixture was then refluxed overnight at the controlled temperature,  $110^\circ C$  and room temperature (RT), under argon ambient. The progress and completion of the reaction were monitored by Thin-layer chromatography (TLC) that was visualized under a UV lamp at 50 Hz. TLC monitoring was done every 30 minutes with pyrocatechol used as the standard. The depletion by the times of pyrocatechol in the refluxed mixture can be calculated by reflecting the consumption of pyrocatechol and the completion of the reaction. The resulting precipitates were washed with a mixture of dioxane (100 mL) and diethyl ether ( $Et_2O$ ) (140 mL) and let to recrystallize under an ice-water bath to form a white or pale precipitate. The precipitate was filtered and washed with  $Et_2O$  (100 mL) under a vacuum. The excess pyrocatechol was removed from the precipitate by rinsing with acetone. Subsequently, the precipitate was dissolved in ethyl acetate (EtOAc) (100 mL) and dehydrated with anhydrous  $Na_2SO_4$ . After the removal of hydrated  $Na_2SO_4$ , the solution was dried with a rotary evaporator. The resulted precipitate was then washed three times with hexane and dried in a vacuum condition. The product was kept in a desiccator until the constant weight was achieved. The composition of the product was investigated using the  $^1H$ -Nuclear magnetic resonance using methanol- $d_4$  as the solvent.

The synthesis reaction can be drawn as scheme 1.

## RESULTS AND DISCUSSION

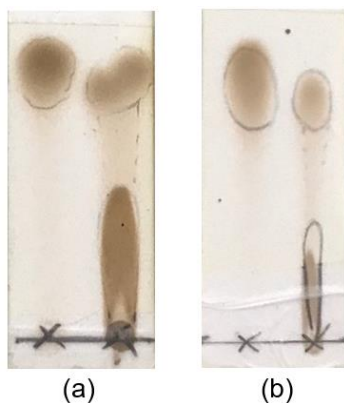
The synthesis of disodium triscatecholates using the pyrocatechol and sodium silicate was successfully achieved at room temperature and high temperature ( $110^\circ C$ ). The reaction was also tested at a higher concentration of starting agents to achieve a higher yield.



**Scheme 1.** The reaction scheme of pyrocatechol and sodium silicate yielding disodium triscatecholate.

## 1. High-Temperature Synthesis (110°C)

Figure 1 shows the TLC results at 3 hours and overnight, respectively. The first lane is spotted the pyrocatechol and the other is the product mixture. The separation of TLC (Figure 1a) indicated the product formation after 3 hours. The consistency depletion of the pyrocatechol in the product mixture at the second lane reflected the completion of the reaction after refluxing overnight (Figure 1b).



**Figure 1.** TLC results of the refluxing mixture at the reaction time of (a) 3 h (b) overnight

The product was recrystallized in the ice bath and washed with EtOAc. White precipitates were collected and characterized using the  $^1\text{H-NMR}$  spectrum. The well-separated double quartet peak of triscatecholate was found for the chemical shift's increments (in ppm) at 6.4-6.55 (see Figure 5(b)).



**Figure 2.** The off-white precipitate of the product produced at 110°C

The reaction scheme between pyrocatechol and sodium silicate can be drawn as shown in Scheme 1. The equivalent ratio of pyrocatechol and sodium silicate is 3:1 while the ratio between pyrocatechol and sodium silicate used in this work was 2.57:1. Therefore, pyrocatechol is the limiting agent in the synthesis. Disodium silicon triscatecholate,  $\text{Na}_2[\text{Si}(\text{catecholate})_3]$ , comprises the centered silicon atom forming six coordinated Si-O bonding and silicon bears with (-2) electronic charges. The number of the hydrogen atom of triscatecholate is 12 atoms/molecule.

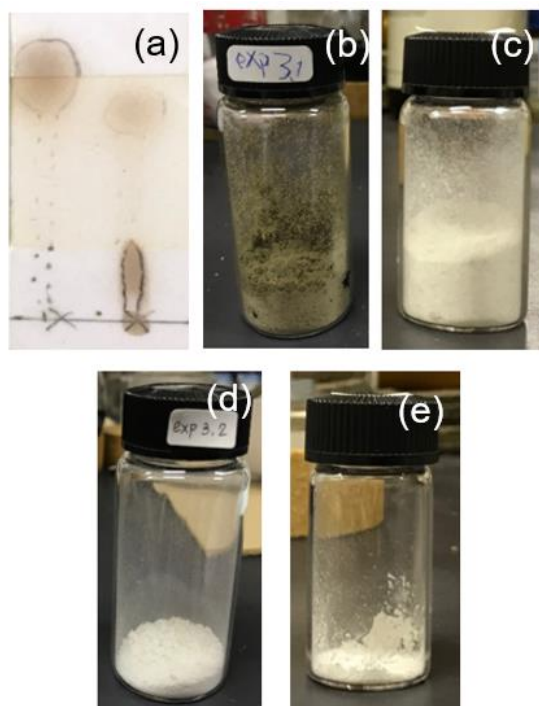
## 2. Room Temperature Synthesis

The experiment was done at room temperature to verify the possibility of energy-saving purposes. The TLC results showed the formation of the product in 3 hours. However, the crystallized product was contaminated, and the solution color was green as shown in Figure 3(b). The crude product must be further treated to remove the impurities. The recrystallization of the crude product using hexane delivered the white precipitate as shown in Figure 3(c).

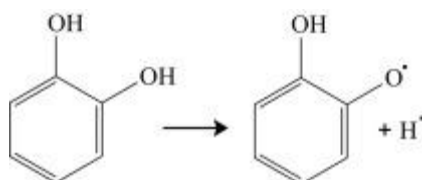
The product in the filtrate was also crystallized to yield the white precipitate shown in Figures 3(d) and 3(e). All precipitates were tested with  $^1\text{H-NMR}$  and the double quartet peaks at  $\delta = 6.4-6.55$ , along with  $\delta = 6.6-6.8$  indicating the partial formation of triscatecholates in the precipitate. Hence, it can be said that the hydrolysis reaction can be developed even at room temperature. The completion of the reaction requires a higher temperature.

Further investigation indicated that the greenish color of the products (Figure 3(b)) was attributed to the oxidation of the pyrocatechol and yielded many colorized products, implying the formation of the by-product [17,18,19]. Figure 4 showed the cleavage of -OH bonding and the form of the hydrogen radical that performs a variety of propagation reactions and yields various visible colors [18]. Moreover, Figure 4 also shows the reactive acidic property of pyrocatechol. The radical of semiquinone is reactive and is able to undergo reactions in many pathways [20]. Eventually, the side reactions performed in this study can be attributed to the various products from the semiquinone.

The  $^1\text{H-NMR}$  spectra of the selected products were elucidated and confirmed the formation of sodium triscatechol (Table 1 and Figure 5).



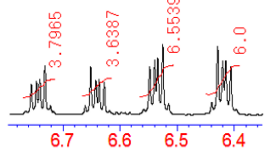

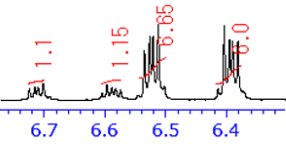

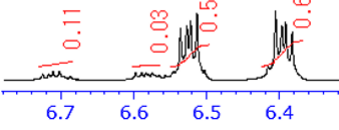

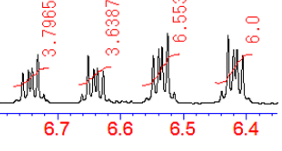

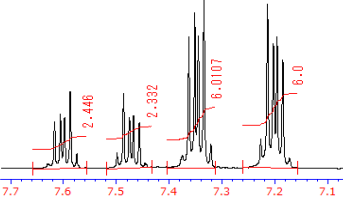

**Figure 3.** Products from the reaction at room temperature (a) TLC results at the equilibrium; (b) The greenish crude product; (c) The white products after recrystallized; (d) and (e) the recrystallized product from the filtrate



**Figure 4.** Scheme of the hydrolysis reaction of pyrocatechol [18]

**Table 1.** <sup>1</sup>H-NMR at 400 MHz of pyrocatechol and the products yielded from the various conditions.

Replicate	Conditions	Signal		Spectrum	Note
		6.4-6.55 (q)	6.7-6.9 (q)		
A	Pyrocatechol	×	✓		
B	0.7247 mol/L pyrocatechol 0.2800 mol/L of Na <sub>2</sub> SiO <sub>3</sub> 110°C, overnight	✓	×		

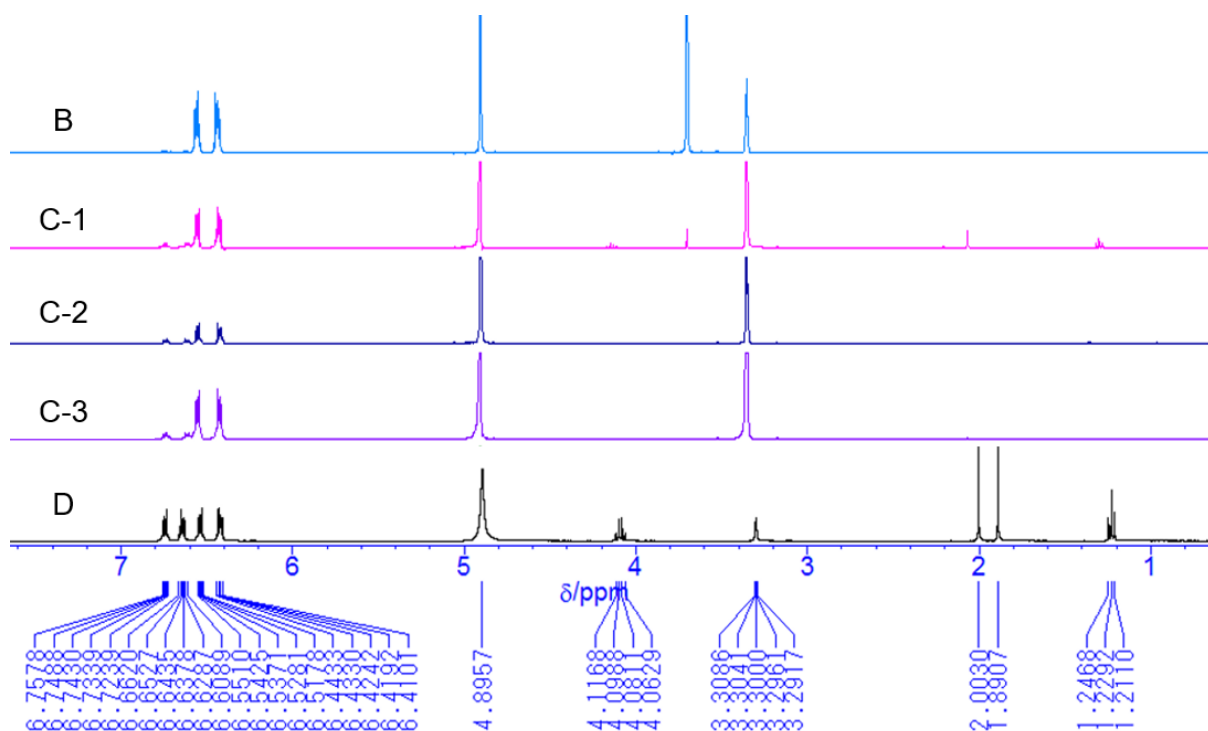
Replicate	Conditions	Signal		Spectrum	Note
		6.4-6.55 (q)	6.7-6.9 (q)		
C-1		✓	✓		
C-2	0.7247 mol/L Pyrocatechol 0.2800 mol/L of Na <sub>2</sub> SiO <sub>3</sub> Room Temperature, overnight	✓	✓		
C-3		✓	✓		
D	2.7338 mol/L Pyrocatechol 1.0526 mole/L of Na <sub>2</sub> SiO <sub>3</sub> 110°C, overnight	✓	✓		
E	By-product (Black color)	×	×		

### 3. High Concentration of Reactants Conditions

The reaction condition using high reactant concentrations was performed with 1.0526 mol/L of sodium silicate and 2.7338 mol/L of pyrocatechol, which is about 3.7 times higher than the low reactant concentration. The reaction proceeded at 110°C and overnight reflux time. Along the reaction time, the colorful mixture during the reflux was observed. The solution changed to red, red wine, and finally, deep brown indicating the side reaction of pyrocatechol. The pyrocatechol was presumed to be hydrolyzed and form various color products such as the blue trace of 1,2,4-trihydroxy benzene, the pink trace of 1,2,3-trihydroxy benzene, the green trace of cis, cis-muconic

acid, the gray trace of maleic acid, the dark blue trace of oxalic acid, and the purple trace of glyoxylic acid [21]. It was attributed to the inadequate water that is necessary for the electron transfer in the formation of Si-O bonding [22].

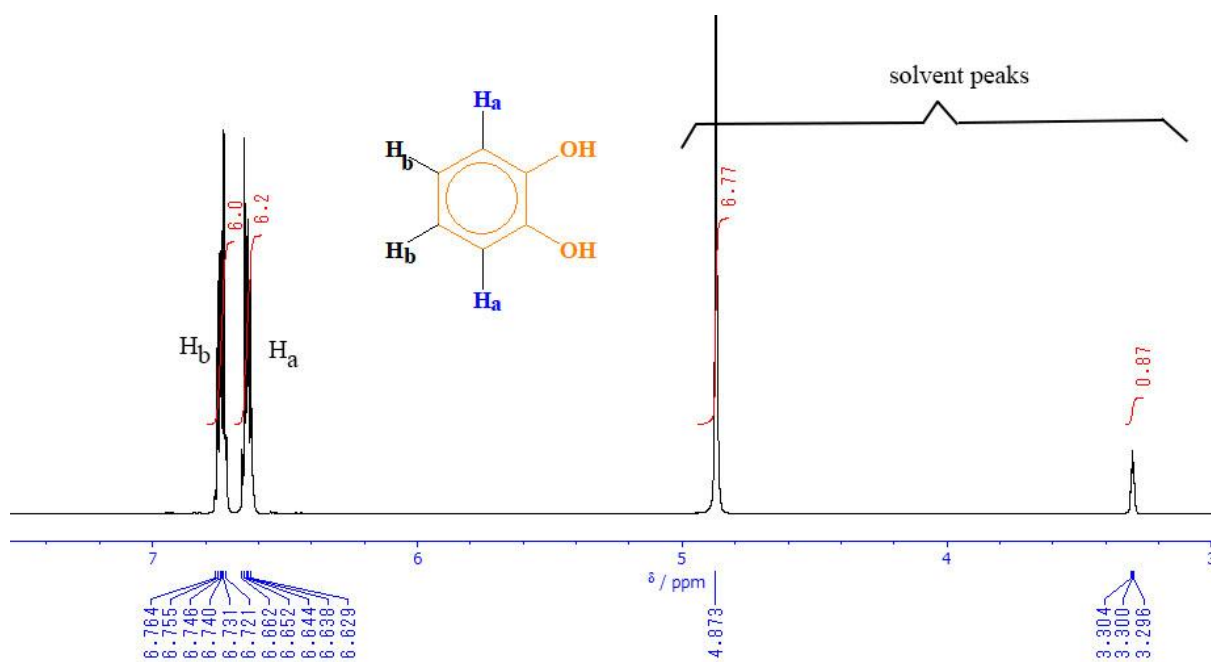
The products of certain batches labeled in Table 1 were selected and monitored. The NMR spectrum is shown in Figure 5 where the product of Na<sub>2</sub>[Si(catecholate)<sub>3</sub>] performed at the shift range of NMR at 6.4 – 6.5 ppm while pyrocatechol was at 6.6–6.7. Solvents used for extraction and washing processes like acetone, methanol, dioxane, and water were also found at 2.0, 3.3, 3.6, and 4.8 ppm respectively.



**Figure 5.**  $^1\text{H-NMR}$  spectrum of the products synthesized (B) Condition: 0.7247 mole/L pyrocatechol, 0.2800 mole/L of  $\text{Na}_2\text{SiO}_3$  at  $110^\circ\text{C}$  (C) 0.7247 mole/L Pyrocatechol, 0.2800 mole/L of  $\text{Na}_2\text{SiO}_3$  at room temperature (D) 2.7338 mole/L Pyrocatechol, 1.0526 mole/L of  $\text{Na}_2\text{SiO}_3$  at  $110^\circ\text{C}$

The  $^1\text{H-NMR}$  spectra in Figure 5 were consistent with the reaction condition in Table 1. It is noted that the product obtained at  $110^\circ\text{C}$  had a clear peak of triscatecholate, whilst the products at room temperature were contaminated with impurities where

the chemical shift of pyrocatechol at  $\delta = 6.6\text{--}6.8$  was observed. Some unknown impurities also responded at  $\delta = 7.1\text{--}7.7$ , which were the contaminated products yielded from the reaction under the deficient amount of water.



**Figure 6.**  $^1\text{H-NMR}$  spectrum of pyrocatechol in  $\text{CD}_3\text{OD}$

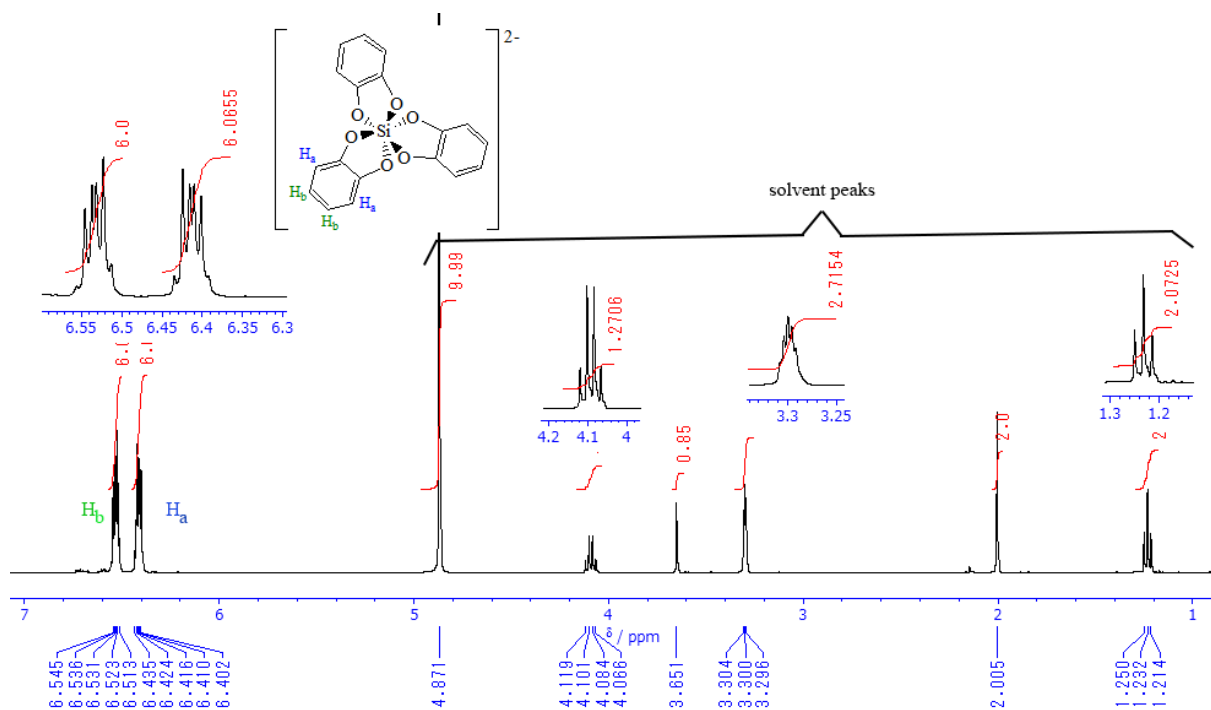


Figure 7. <sup>1</sup>H-NMR spectrum of pyrocatechol in CD<sub>3</sub>OD

The interpretation of the <sup>1</sup>H-NMR spectrum was also included to clarify the characteristic of the pyrocatechol and the product as followed. Figure 6 shows <sup>1</sup>H-NMR of pyrocatechol performed with multiple signals at  $\delta = 6.64$  (m, 2H<sub>a</sub>),  $\delta = 6.74$  (m, 2H<sub>b</sub>). The ortho proton (H<sub>a</sub>) was influenced by the electron of oxygen in the hydroxyl group [23] and appeared upfield region. The proton integration suggested the ratio of H<sub>a</sub>: H<sub>b</sub> is 1:1, which corresponds to protons in pyrocatechol. It should be mentioned here that OH is never showing the absorption in the vicinity of CD<sub>3</sub>OD. It was attributed to the exchange between deuterium and proton in OH and the peaks shrunk or disappeared entirely [24]. Figure 7 presents the <sup>1</sup>H-NMR of the product contaminated with the solvent used in the synthesis process such as ethyl acetate ( $\delta = 4.2$  and 2.05) and diethyl ether ( $\delta = 1.25$ ).

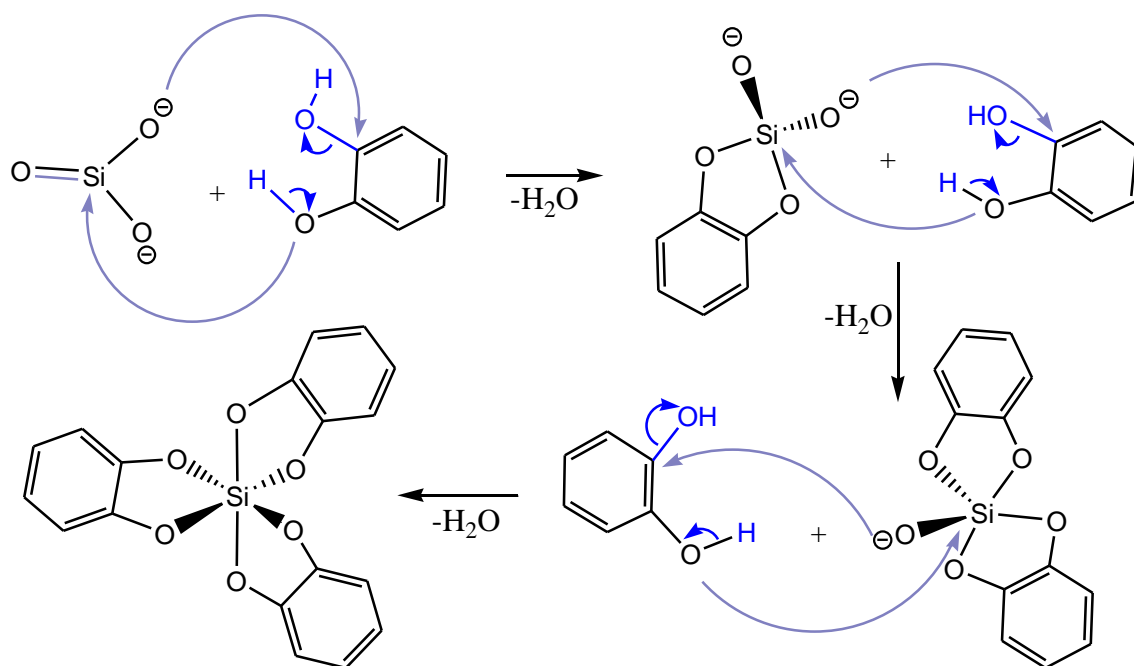
There are the absorption peaks for H<sub>a</sub> at 6.402-6.435 ppm with the integrated proton of 6.1 and H<sub>b</sub> at 6.513-6.545 ppm with the same ratio of the integrated proton. The overall integration of H<sub>a</sub> and H<sub>b</sub> of the product is 6: 6 suggesting the completion of six coordinated bonds at the silicon center atom by the bidentate of catechol, which means that the valence orbitals are sp<sup>3</sup>d<sup>2</sup> hybridized. The geometry of the silicon in this compound is an octahedral shape and geometry [25]. This spectrum is well-agree with the

study of Corey D. Pilgrim (2018). Then, it can be concluded that the product of this study is silicon triscatecholate [26].

#### 4. The Reaction Schemes

To understand the reactivity pattern of the organo-silicon complex, it is essential to get deep into some specific properties. Silicon has an atomic number of 14 and lies beneath carbon in the modern periodic table. The silicon compound mostly forms four bonds using sp<sup>3</sup> atomic orbital hybridization with a tetrahedral structure. Silicon can extend the coordination number beyond four and imparts unique property and its reactivity pattern. The hypervalent bonding implies a transfer of the electrons from the silicon central atom to the nonbonding molecular orbitals, which it forms with the oxy ligand [27].

The aqueous sodium silicate generally exists in planar geometry as shown in Figure 8 (top) [28]. The complexation reaction follows a similar reaction pathway, that of a simple condensation reaction as shown in Figure 8. Surrounding with oxygen, silicon possesses the electron deficiency characteristic, then form the coordinate covalent with oxygen from catecholate and removes one molecule of water. The reaction proceeds with another two catecholate ions and forms the triscatecholate ion.



**Figure 8.** The proposed scheme of the reaction

Herein, in this work, the formation of disodium triscatecholate using simple silica reacted with pyrocatechol was accomplished. The finding can be used as an alternative synthesis method that provides a lower cost of the silicate precursor and supports the biomimetic approach inspired by natural metal binders in biomedical engineering.

#### CONCLUSION

In this work, the synthesis of triscatecholates as valuable multivalent anchor molecules was achieved. Disodium silicon triscatecholate was managed to be synthesized at 110°C and room temperature. The effects of the precursor concentration were also investigated.

The signal of triscatecholates presence in the product at both 110°C and room temperature indicated that the disodium triscatecholates were successfully synthesized from silica under an argon environment. At the reaction temperature of 110°C, the concentration of the precursors influences the equilibration time and stability of the silicon triscatecholate derivatives. However, the reaction at the higher temperature yielded higher product purity at the equilibration conditions when compared with the reaction at room temperature. It is also found that water played an important role as the necessary medium that supports the removal of hydrogen atoms from pyrocatechol. These catecholate anchors produced by the low cost of silica would be an alternative used as effector-catecholate conjugates for the generation of a bio passive approach and have the versatility of the developed approach in the future.

#### ACKNOWLEDGMENTS

The authors would like to express the special thanks of gratitude to Prof. Yoshio Kabe, Kanagawa University Japan, who gave us the golden opportunity to do this wonderful project including support from all the facilities on this research that encouraged us to gain much experience in Japan.

#### CONFLICT OF INTEREST STATEMENT

The authors agree that this research was conducted in the absence of any self-benefits, commercial or financial conflicts and declare the absence of conflicting interests with the funders.

#### REFERENCES

- Hahn, F. E., Keck, M. & Raymond, K. N. (1995) Catecholate Complexes of Silicon: Synthesis and Molecular and Crystal Structures of [Si(cat)<sub>2</sub>]. 2THF and Li<sub>2</sub>[Si(cat)<sub>3</sub>]. *Inorganic Chemistry*, **34**(6), 1402–1407. <https://doi.org/10.1021/ic00110a018>
- Klitsche, F., Ramcke, J., Migenda, J., Hensel, A., Vossmeier, T., Weller, H., Gross, S. & Maison, W. (2015) Synthesis of tripodal catecholates and their immobilization on zinc oxide nanoparticles. *Beilstein Journal of Organic Chemistry*, **11**, 678–686. <https://doi.org/10.3762/bjoc.11.77>
- Sakib, S., Bakhshandeh, F., Saha, S., Soleymani, L. & Zhitomirsky, I. (2021) Surface Functionalization of Metal Oxide Semiconductors with Catechol



- Ligands for Enhancing Their Photoactivity. *Solar RRL*, **5**(10), 2100512. <https://doi.org/10.1002/solr.202100512>
4. Franzmann, E., Khalil, F., Weidmann, C., Schröder, M., Rohnke, M., Janek, J., Smarsly, B. M. & Maison, W. (2011) A Biomimetic Principle for the Chemical Modification of Metal Surfaces: Synthesis of Tripodal Catecholates as Analogues of Siderophores and Mussel Adhesion Proteins. *Chemistry – A European Journal*, **17**(31), 8596–8603. <https://doi.org/10.1002/chem.201100715>
  5. Kawakami, Y., Ogishima, T., Kawara, T., Yamauchi, S., Okamoto, K., Nikaido, S., Souma, D., Jin, R.-H. & Kabe, Y. (2019) Silane catecholates: Versatile tools for self-assembled dynamic covalent bond chemistry. *Chemical Communications*, **55**(43), 6066–6069. <https://doi.org/10.1039/C9CC02103E>
  6. Broomell, C. C., Mattoni, M. A., Zok, F. W. & Waite, J. H. (2006) Critical role of zinc in hardening of Nereis jaws. *The Journal of Experimental Biology*, **209**(16), 3219–3225. <https://doi.org/10.1242/jeb.02373>
  7. Xu, Z. (2013) Mechanics of metal-catecholate complexes: The roles of coordination state and metal types. *Scientific Reports*, **3**(1), 2914. <https://doi.org/10.1038/srep02914>
  8. Diffels, J. F., Seret, M. -L., Goffeau, A. & Baret, P. V. (2006) Heavy metal transporters in Hemiascomycete yeasts. *Biochimie*, **88**(11), 1639–1649. <https://doi.org/10.1016/j.biochi.2006.08.008>
  9. Wu, H., Zhang, C., Liang, Y., Shi, J., Wang, X. & Jiang, Z. (2013) Catechol modification and covalent immobilization of catalase on titania submicrospheres. *Journal of Molecular Catalysis B: Enzymatic*, **92**, 44–50. <https://doi.org/10.1016/j.molcatb.2013.03.018>
  10. Petrov, P. A., Filippova, E. A., Eltsov, I. V., Sukhikh, T. S., Piskunov, A. V. & Sokolov, M. N. (2021) Catecholate derivatives of zirconocene: Facile methylation of a catecholate ring. *Journal of Organometallic Chemistry*, **949**, 121946. <https://doi.org/10.1016/j.jorganchem.2021.121946>
  11. Heggemann, S., Möllmann, U., Gebhardt, P. & Heinisch, L. (2003) Trishydroxamates and triscatecholates based on monosaccharides and myo-inositol as artificial siderophores. *Biometals: An International Journal on the Role of Metal Ions in Biology, Biochemistry, and Medicine*, **16**(4), 539–551. <https://doi.org/10.1023/a:1023476214838>
  12. Wittmann, S., Heinisch, L., Scherlitz-Hofmann, I., Stoiber, T., Ankel-Fuchs, D. & Möllmann, U. (2004) Catecholates and mixed catecholate hydroxamates as artificial siderophores for mycobacteria. *Biometals: An International Journal on the Role of Metal Ions in Biology, Biochemistry, and Medicine*, **17**(1), 53–64. <https://doi.org/10.1023/a:1024409517626>
  13. Han, A. W., Sandy, M., Fishman, B., Trindade-Silva, A. E., Soares, C. A. G., Distel, D. L., Butler, A. & Haygood, M. G. (2013) Turnerbactin, a Novel Triscatecholate Siderophore from the Shipworm Endosymbiont *Teredinibacter turnerae* T7901. *PLoS ONE*, **8**(10), e76151. <https://doi.org/10.1371/journal.pone.0076151>
  14. Ye, X., Zhou, Y., Sun, Y., Chen, J. & Wang, Z. (2008) Structure and infrared emissivity of collagen/SiO<sub>2</sub> composite. *Applied Surface Science*, **254**(18), 5975–5980. <https://doi.org/10.1016/j.apsusc.2008.03.186>
  15. Perumal, S., Ramadass, S. K., Gopinath, A., Madhan, B., Shanmugam, G., Rajadas, J. & Mandal, A. B. (2015) Altering the concentration of silica tunes the functional properties of collagen-silica composite scaffolds to suit various clinical requirements. *Journal of the Mechanical Behavior of Biomedical Materials*, **52**, 131–138. <https://doi.org/10.1016/j.jmbmm.2015.04.006>
  16. Kingston, J. V., Vargheese, B. & Sudheendra Rao, M. N. (2000) Synthesis and Characterization of Tris(catecholato)Silicates, [(C<sub>6</sub>H<sub>4</sub>O<sub>2</sub>)<sub>3</sub>Si]<sup>2-</sup> with Different Counter Cations – First Pyrolysis Study and X-ray Structure of [(CH<sub>3</sub>)<sub>2</sub>CH]<sub>2</sub>NH<sub>2</sub>[(C<sub>6</sub>H<sub>4</sub>O<sub>2</sub>)<sub>3</sub>Si] · 2CH<sub>3</sub>CN.H<sub>2</sub>O. *Main Group Chemistry*, **3**(2), 79–90. <https://doi.org/10.1080/13583140012331339039>
  17. Baker, W. (1934) The condensation of catechol with acetone. *Journal of the Chemical Society*, **1934**, 1678–1681. <https://doi.org/10.1039/JR9340001678> <https://doi.org/10.3390/molecules26123548>
  18. Schweigert, N., Zehnder, A. J. B. & Eggen, R. I. L. (2001) Chemical properties of catechols and their molecular modes of toxic action in cells, from microorganisms to mammals. *Environmental Microbiology*, **3**(2), 81–91. <https://doi.org/10.1046/j.1462-2920.2001.00176.x>
  19. Moldoveanu, S. C. (2019) Chapter 4—Pyrolysis of Alcohols and Phenols. In S. C. Moldoveanu (Ed.), *Pyrolysis of Organic Molecules (Second Edition)*, Elsevier, 207–278. <https://doi.org/10.1016/B978-0-444-64000-0.00004-4>

20. Chen, S. -H. & Li, C. -W. (2019) Detection and Characterization of Catechol Quinone-Derived Protein Adducts Using Biomolecular Mass Spectrometry. *Frontiers in Chemistry*, **7**, 571. <https://doi.org/10.3389/fchem.2019.00571>
21. Pillar-Little, E., Zhou, R. & Guzman, M. (2015) Heterogeneous Oxidation of Catechol. *The Journal of Physical Chemistry A*, **119**. <https://doi.org/10.1021/acs.jpca.5b07914>
22. Sugumaran, M. (2016) Reactivities of Quinone Methides versus o-Quinones in Catecholamine Metabolism and Eumelanin Biosynthesis. *International Journal of Molecular Sciences*, **17**, 1576. <https://doi.org/10.3390/ijms17091576>
23. Wishart, D. S., Knox, C., Guo, A. C., Eisner, R., Young, N., Gautam, B., Hau, D. D., Psychogios, N., Dong, E., Bouatra, S., Mandal, R., Sinelnikov, I., Xia, J., Jia, L., Cruz, J. A., Lim, E., Sobsey, C. A., Shrivastava, S., Huang, P., Forsythe, I. (2009) HMDB: A knowledgebase for the human metabolome. *Nucleic Acids Research*, **37**, D603–D610 (Database). <https://doi.org/10.1093/nar/gkn810>
24. Chemistry LibreTexts (2015) *Spectroscopy of Alcohols and Phenols*, **17(11)**. [https://chem.libretexts.org/Bookshelves/Organic\\_Chemistry/Organic\\_Chemistry\\_\(McMurry\)/17%3A\\_Alcohols\\_and\\_Phenols/17.11%3A\\_Spectroscopy\\_of\\_Alcohols\\_and\\_Phenol](https://chem.libretexts.org/Bookshelves/Organic_Chemistry/Organic_Chemistry_(McMurry)/17%3A_Alcohols_and_Phenols/17.11%3A_Spectroscopy_of_Alcohols_and_Phenol)
25. Kinrade, S. D., Del Nin, J. W., Schach, A. S., Sloan, T. A., Wilson, K. L. & Knight, C. T. G. (1999) Stable Five- and Six-Coordinated Silicate Anions in Aqueous Solution. *Science*, **285(5433)**, 1542–1545. <https://doi.org/10.1126/science.285.5433.1542>
26. Pilgrim, C., Colla, C., Ochoa, G., Walton, J. & Casey, W. (2018) <sup>29</sup>Si NMR of aqueous silicate complexes at gigapascal pressures. *Communications Chemistry*, **1**, 67. <https://doi.org/10.1038/s42004-018-0066-3>
27. Singh, G., Kaur, G. & Singh, J. (2018) Progressions in hyper-coordinate silicon complexes. *Inorganic Chemistry Communications*, **88**, 11–20. <https://doi.org/10.1016/j.inoche.2017.12.002>
28. Ebnesajjad, S. (2011) Characteristics of Adhesive Materials. In S. Ebnesajjad (Ed.), *Handbook of Adhesives and Surface Preparation*, William Andrew Publishing, 137–183. <https://doi.org/10.1016/B978-1-4377-4461-3.10008-2>